

# The Mechanistic Study of Methane Reforming with Carbon Dioxide on Ni/α-Al<sub>2</sub>O<sub>3</sub>

V. Yu. Bychkov, O. V. Krylov, and V. N. Korchak

*Semenov Institute of Chemical Physics, Russian Academy of Sciences, Moscow, 117977 Russia*

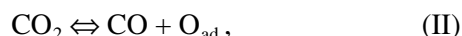
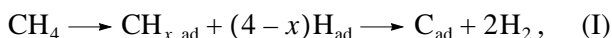
Received October 25, 2000

**Abstract**—The reactions of oxidized and reduced 6 wt % NiO/α-Al<sub>2</sub>O<sub>3</sub> with H<sub>2</sub>, CH<sub>4</sub>, CO<sub>2</sub>, O<sub>2</sub>, and their mixtures are studied in flow and pulse regimes using a setup equipped with a differential scanning calorimeter DSC-111 and a system for chromatographic analysis. It is shown that treatment with hydrogen at 700°C results in the partial reduction of NiO to Ni. Methane practically does not react with oxidized Ni/α-Al<sub>2</sub>O<sub>3</sub> but it does react actively with the reduced catalyst to form H<sub>2</sub> and surface carbon. The latter is capable of reacting with lattice oxygen of Ni/α-Al<sub>2</sub>O<sub>3</sub> (slowly) and with adsorbed oxygen (rapidly). Carbon dioxide also reacts with surface carbon to form CO (rapidly) and with metallic Ni to yield CO and NiO (slowly). Thus, the main route of methane reforming with carbon dioxide on Ni/α-Al<sub>2</sub>O<sub>3</sub> is the dissociative adsorption of CH<sub>4</sub> to form surface carbon and H<sub>2</sub> and the reaction of this carbon with CO<sub>2</sub> resulting in the formation of CO by the reverse Boudouard reaction. Side routes are the interaction of the products of methane chemisorption with catalyst oxygen and the dissociative adsorption of CO<sub>2</sub> on metallic nickel. A competitive reaction of surface carbon with adsorbed oxygen results in a decrease in the CO<sub>2</sub> conversion in methane reforming with carbon dioxide. Therefore, the presence of gaseous oxygen in the reacting mixture decelerates methane reforming (catalyst poisoning by oxygen).

## INTRODUCTION

Methane reforming with carbon dioxide is a promising method for syngas manufacturing. Platinum-group metals and nickel are suitable catalysts for this process. Various characteristics of these catalysts were discussed in detail in review papers [1, 2]. However, the optimization of catalyst performance and reaction conditions is far from being completed. In connection with this, further mechanistic and kinetic studies of methane reforming with carbon dioxide remain a topical problem.

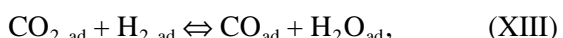
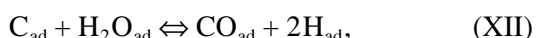
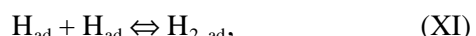
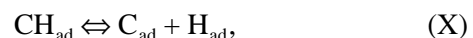
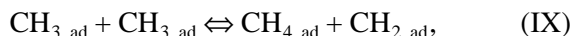
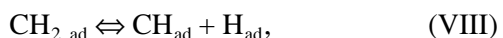
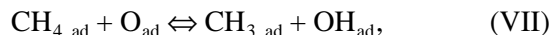
Most mechanisms proposed for carbon dioxide reforming [1, 2] assume the dissociative adsorption of methane (reaction (I)). Then, the consecutive dissociation of CH<sub>4</sub> to form the CH<sub>x</sub> and C species on the surface is considered. These species react with adsorbed oxygen atoms (reaction (III)), which are formed by the reaction of CO<sub>2</sub> with the metal surface (reaction (II)):



In some papers [3], the activation of CO<sub>2</sub> is assumed to occur via the direct reaction with surface carbon by the reverse Boudouard reaction:



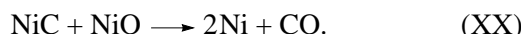
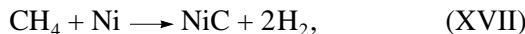
In more recent publications, mechanisms proposed for methane reforming with carbon dioxide consider more details. One of the most detailed schemes was proposed in [4]:



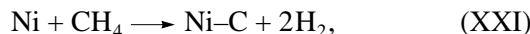
In this scheme, the dissociative activation of methane (I) is viewed as a five-step process (reactions (VI), (VIII)–(X)). Additionally, methane can be activated by reaction (VII) with adsorbed oxygen. Carbon dioxide activation can occur via dissociative adsorption (XIV), reaction with adsorbed carbon (XV) and adsorbed hydrogen (XIII). However, this overcomplicated scheme, which involves several routes for methane and

$\text{CO}_2$  activation, does not address the question of which routes are of primary and secondary importance. Therefore, it is still to be determined what routes of carbon dioxide reforming are decisive for different catalysts and reaction conditions.

It has been shown [1, 2] that, when the active component (Ni or Pt) is supported on materials that strongly adsorb  $\text{CO}_2$ , additional routes leading to the products may appear in carbon dioxide reforming. For instance, in the case of catalysts containing lanthanum, magnesium, and zirconium oxides, there is a route for  $\text{CO}_2$  activation via the formation of metal carbonates, which further react to form CO [5]:

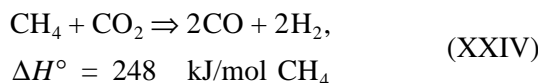


Several researchers [6, 7] proposed that the introduction of transition metals also creates additional routes for methane and  $\text{CO}_2$  activation to form CO and  $\text{H}_2$ , e.g., [6]:



Data reported in such publications are inconclusive regarding the question of whether these additional routes are fast enough to contribute to an increase in the overall rate of methane reforming with carbon dioxide. An apparent increase in the catalytic activity is possibly determined by the creation of better conditions for the occurrence of reforming via the main mechanism due to the suppression of coking, an increase in the active surface area of metallic particles, and other factors, and is not determined by the formation of CO and  $\text{H}_2$  via additional routes.

The role of reactions that involve active oxygen in the mechanism of methane reforming with carbon dioxide remains poorly studied, although information on the effect of gas-phase and lattice oxygen on the rate and selectivity of reforming is important, because the addition of oxygen to the reaction mixture and the partial oxidation of methane may theoretically compensate for the strong endothermic effect of the reaction



and make it acceptable for commercial use. However, there are restrictions due to thermodynamics and the specific features of the mechanism of coupled reactions (XXIV) and methane oxidation.

Earlier, we showed for the complete oxidation of methane [8], the oxidative coupling of methane [9], and

the oxidative dehydrogenation of paraffins [10] that new mechanistic data can be obtained when the studies of catalyst interactions with reactive mixtures and their separate components under nonstationary conditions are coupled with chromatographic analysis and measuring the heat evolved in the reaction zone. Therefore, the goal of this work was to study the interaction of  $\text{Ni}/\alpha\text{-Al}_2\text{O}_3$ , which is one of the well-known systems, with separate gases  $\text{CH}_4$ ,  $\text{CO}_2$ , CO,  $\text{O}_2$ ,  $\text{H}_2$ , and the  $\text{CH}_4 + \text{CO}_2$  mixture to shed some light on the problems mentioned above. We gave special attention to the role of active oxygen in the process of methane reforming with carbon dioxide.

## EXPERIMENTAL

A 6 wt %  $\text{NiO}/\alpha\text{-Al}_2\text{O}_3$  sample (henceforth denoted as  $\text{Ni}/\text{Al}_2\text{O}_3$ ) was prepared by alumina (Catalyst & Chemical Europe, s.a., 35  $\text{m}^2/\text{g}$ ) impregnation with nickel nitrate. Details of the procedure were reported earlier [6].

The interaction of the sample with gaseous reactants was studied using a setup that involves a differential scanning calorimeter DSC-111 and two gas chromatographs. The sample (150 mg) was loaded into a flow-type quartz cell, which was placed into the measurement channel of the calorimetric block of DSC-111. The sample pretreatment included heating in a flow of air at 700°C for 60 min. For the study of the reduced catalyst, the sample was treated in a flow of the 10%  $\text{H}_2$ -He mixture at 700°C for 30 min. The interaction of the sample with the reactants was studied in flow or pulse regimes. In the case of a pulse regime, a flow of specially purified helium passed through the sample with a flow rate of 30 ml/min. Pulses of reactive gases (0.5 ml) were added to the helium flow using a six-way valve. The flow passed through the sample and then was analyzed consecutively in two chromatographic columns packed with Porapak N and zeolite 5A using a thermal-conductivity detector. The system for analysis allowed us to measure the concentrations of  $\text{CO}_2$ ,  $\text{H}_2$ ,  $\text{O}_2$ ,  $\text{N}_2$ ,  $\text{CH}_4$ , CO,  $\text{C}_2\text{H}_6$ , and  $\text{C}_2\text{H}_4$ . In the case of the pulse supply of reactants, the concentrations of the components of the mixture were calculated in volume percents relative to the volume of the initial pulse.

XRD analyses were carried out using a DRON-3 instrument with  $\text{CuK}_\alpha$  irradiation. The specific surface area was measured using the low-temperature adsorption of nitrogen.

## RESULTS

**Phase composition.** X-ray diffraction patterns of the  $\text{Ni}/\text{Al}_2\text{O}_3$  sample show the intense signals of  $\alpha\text{-Al}_2\text{O}_3$  and the low-intensity signals of  $\gamma\text{-Al}_2\text{O}_3$ . No signals were found that corresponded to  $\text{NiO}$  or  $\text{NiAl}_2\text{O}_4$ . This proves the high dispersion of supported nickel oxide. Proceeding from the values of a surface area covered by one  $\text{NiO}$  molecule ( $0.0439 \text{ nm}^2$ ), the

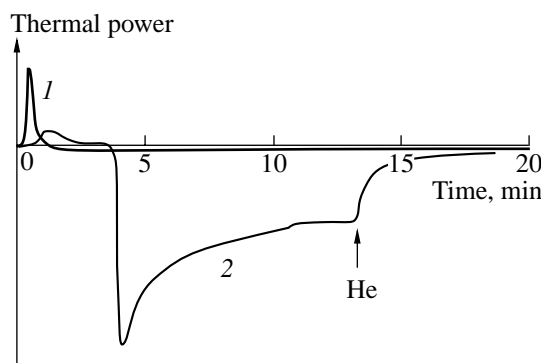


**Fig. 1.** Heat evolution in the reaction of the Ni/Al<sub>2</sub>O<sub>3</sub> sample with a flow of (1) 10% H<sub>2</sub> + He and (2) CH<sub>4</sub>.

monolayer coverage of 6 wt % NiO is achieved when the specific surface area of the support is 21 m<sup>2</sup>/g. Therefore, for the alumina used in this work (35 m<sup>2</sup>/g), the monolayer coverage of NiO was achievable.

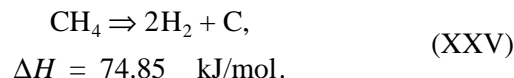
**Interaction with a hydrogen flow.** The oxidized sample can be reduced with hydrogen at 700°C. Figure 1 shows the curve of heat evolution when the flow of helium is switched to the flow of 10% H<sub>2</sub> + He. Intensive heat evolution for 1–2 min points to rapid reduction of nickel oxide. Then, the rate of reduction decreases almost to zero and then remains constant. This kinetics of reduction allowed us to obtain samples with the same extent of reduction (30-min treatment in a flow of hydrogen at 700°C was further used in different runs). The sample thus reduced can be reoxidized by the pulses of air. The rate of reoxidation was also very high (95% conversion of oxygen was observed) and allowed us to measure the amount of oxygen consumed for the reoxidation process and the specific heat of the process (Table 1).

The overall amount of oxygen consumed at 700°C by the oxidized sample was 88 μmol O<sub>2</sub>/g. The initial catalyst contains 803 μmol NiO/g (according to the weight composition: 6% NiO + 94% Al<sub>2</sub>O<sub>3</sub>). Therefore, during treatment with hydrogen (700°C, 30 min), 22% of nickel oxide is reduced.

**Table 1.** Oxygen consumption and heat evolution ( $Q_{ox}$ ) in the reoxidation of prerduced Ni/Al<sub>2</sub>O<sub>3</sub> by air pulses at 700°C

| Pulse number | O <sub>2</sub> conversion, % | $Q_{ox}$ , kJ/mol O <sub>2</sub> |
|--------------|------------------------------|----------------------------------|
| 1            | 95                           | 499                              |
| 2            | 95                           | 472                              |
| 3            | 95                           | 442                              |
| 4            | 58                           | 490                              |
| 5            | 0.16                         | –                                |
| 6            | 0.01                         | –                                |

**Interaction with a flow of methane.** The reduced sample interacts with methane more slowly than with hydrogen. When the oxidized sample interacts with methane pulses at 700°C, CO<sub>2</sub> and the traces of C<sub>2</sub>H<sub>6</sub> are formed. Figure 1 shows a heat-evolution curve for the reaction of the oxidized sample with a flow of methane at 700°C. It can be seen, that the initial heat evolved in the reaction with methane is much lower than the initial heat evolved in the reaction with hydrogen. During the first three minutes, methane interacts with the most reactive oxygen from nickel oxide and forms CO<sub>2</sub> and traces of C<sub>2</sub>H<sub>6</sub>. After 4 min, the conversion of methane drastically increases. Chromatographic data and the apparent intensive consumption of heat indicates the occurrence of the reaction



A gradual decrease in the endothermic effect points to the retardation of reaction (XXV) due to the cocking of the metallic nickel surface. The replacement of the methane flow by helium after 13 min leads to the disappearance of the thermal effect. The reoxidation of such a sample at 700°C is accompanied by the formation of carbon oxides in large amounts.

**Interaction with the pulses of CH<sub>4</sub> + CO<sub>2</sub>.** The oxidized sample practically does not react with CH<sub>4</sub> + CO<sub>2</sub> pulses at 700°C, although the sample reduced by hydrogen exhibits the catalytic activity in syngas formation. Figure 2 shows data on the concentrations of CO<sub>2</sub>, CH<sub>4</sub>, CO, and H<sub>2</sub> (in percent relative to the initial volume of a pulse) in the products of the reaction between the pulses of a 49% CH<sub>4</sub> + 49% CO<sub>2</sub> + 2% N<sub>2</sub> mixture (pulses 1–6) and Ni/Al<sub>2</sub>O<sub>3</sub> pretreated in a flow of H<sub>2</sub> at 700°C. Under the experimental conditions, the constant catalytic activity was observed at CH<sub>4</sub> and CO<sub>2</sub> conversions equal to 65 and 85%, respectively.

Figure 2 also shows that the partial oxidation of the catalyst affects its catalytic activity. Before supplying the pulses of the CH<sub>4</sub> + CO<sub>2</sub> mixture (no. 8 and no. 12), the catalyst was treated by one (no. 8) and three (no. 12) pulses of air and absorbed 2.5 and 4.6 μmol O<sub>2</sub>, which is ~20 and 60% of all oxygen absorbed by the sample in reoxidation. It is seen that sample reoxidation to an extent of 20% results in an increase in the methane conversion and hydrogen yield. However, the conversion of CO<sub>2</sub> and the yield of CO decrease. In the second and further pulses of the CH<sub>4</sub> + CO<sub>2</sub> mixture (pulses no. 9 and no. 10), the concentrations of products become close to the stationary values.

After the deep (60%) oxidation of the catalyst, the yield of hydrogen decreases in the first pulse of the CH<sub>4</sub> + CO<sub>2</sub> mixture (no. 12) but increases in the second and third pulses. The conversion of CO<sub>2</sub> decreases almost to zero. The yield of CO decreases accordingly. In further pulses of the CH<sub>4</sub> + CO<sub>2</sub> mixture the stationary values are also restored.

**Interaction with the pulses of  $\text{CH}_4$ .** Figure 3 shows data on the reaction of the reduced sample with 100%  $\text{CH}_4$  pulses. The conversion of methane remains almost constant for the first 5–6 pulses (there is a slight maximum of the methane conversion at the third pulse, which is unnoticeable at the scale of Fig. 3). Then, the value of methane conversion starts to decrease. During first five pulses, the formation of CO is observed, but  $\text{CO}_2$  is not formed. Figure 4 shows the fragments of chromatograms corresponding to the peaks of methane and CO observed in the sample reduction by the pulses of  $\text{CH}_4$ ,  $\text{CO}_2$ , and  $\text{CH}_4 + \text{CO}_2$ . In the two latter cases, the retention time and the peak widths for CO were determined by the conditions of chromatographic separation in the column. However, the retention time and the peak width of CO are much greater in the case of the  $\text{CH}_4$  pulse. This means that CO formation is retarded in this case.

The formation of hydrogen in the reaction of methane pulses with the reduced sample is maximal for the first pulse (Fig. 3). The amount of  $\text{H}_2$  somewhat decreases in further pulses. There is a slight maximum during the fourth and fifth pulses and a substantial decrease after the sixth pulse. The maximum and the further decrease in the  $\text{H}_2$  yield apparently suggest that the overall conversion of methane changes according to reaction (XXV), because the unnoticeable maximum for methane (not seen in Fig. 3) and the further decrease are observed.

**Interaction with the pulses of  $\text{CO}_2$ .** The only product observed in the reaction of  $\text{CO}_2$  pulses with the reduced sample is CO. This fact points to the occurrence of reaction (II). The dependence of CO formation on the pulse number is shown in Fig. 5. The yield of CO gradually decreases as metallic nickel is reoxidized. It is seen that the conversion of  $\text{CO}_2$  and the yield of CO are an order of magnitude lower in this case than under conditions of the catalytic process on the reduced sample (Fig. 2). Figure 6 shows the heat-evolution curve for the reaction of  $\text{CO}_2$  pulse with the sample at 700°C. The exothermic effect (10–20 s) changes for endothermic (20–50 s), which is equivalent in the amount of heat. The fact that the zero line somewhat lowers at the initial moment is not associated with the endothermic effect. Rather, its lowering is due to physical reasons (a pressure jump and a thermal conductivity change). The shape of the curve points to the existence of noticeable equilibrium adsorption of  $\text{CO}_2$  on the sample. Unlike in reaction (II) of CO formation from  $\text{CO}_2$ , the intensity of equilibrium adsorption was independent of the extent of sample oxidation. The thermal effect of equilibrium adsorption prevented us from measuring the heat of reaction (II) under the experimental conditions.

**Interaction with the pulses of  $\text{CH}_4$  and  $\text{CO}_2$ .** For a more detailed study of the mechanism of  $\text{CO}_2$  drawing in methane conversion, we carried out experiments with alternating  $\text{CH}_4$  and  $\text{CO}_2$  pulses. Figure 7 shows

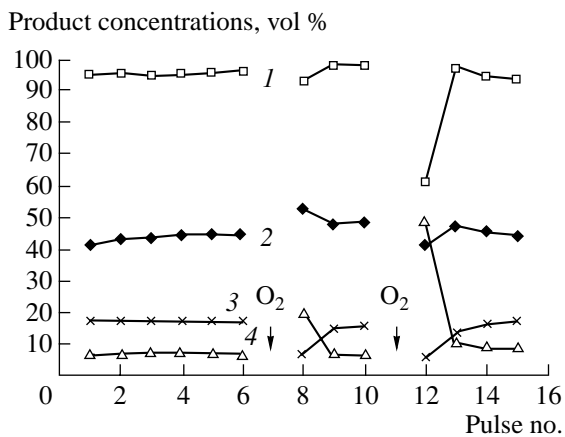


Fig. 2. The concentration of (1) CO, (2)  $\text{H}_2$ , (3)  $\text{CH}_4$ , and (4)  $\text{CO}_2$  in the products of the reaction between the pulses of  $\text{CH}_4 + \text{CO}_2$  and reduced  $\text{Ni}/\text{Al}_2\text{O}_3$  at 700°C.

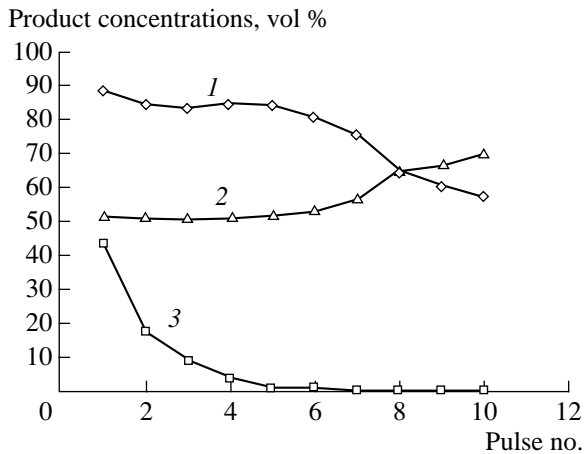


Fig. 3. The concentration of (1)  $\text{H}_2$ , (2)  $\text{CH}_4$ , and (3) CO in the products of the reaction between the pulses of 100%  $\text{CH}_4$  and reduced  $\text{Ni}/\text{Al}_2\text{O}_3$  at 700°C.

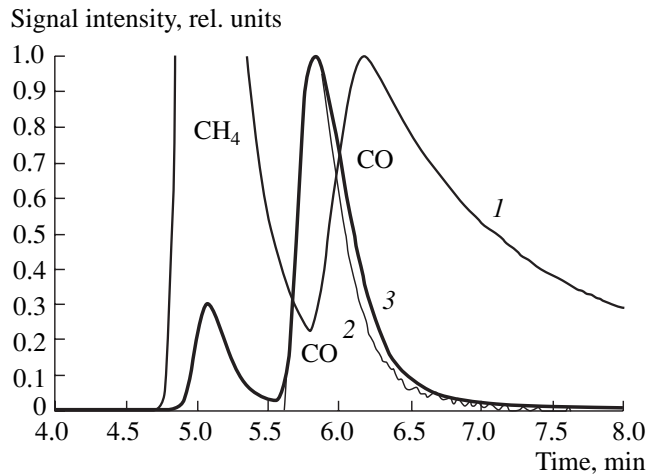


Fig. 4. Chromatograms of the reaction products in the reaction of  $\text{Ni}/\text{Al}_2\text{O}_3$  with the pulses of (1)  $\text{CH}_4$ , (2)  $\text{CO}_2$ , and (3)  $\text{CH}_4 + \text{CO}_2$  at 700°C.

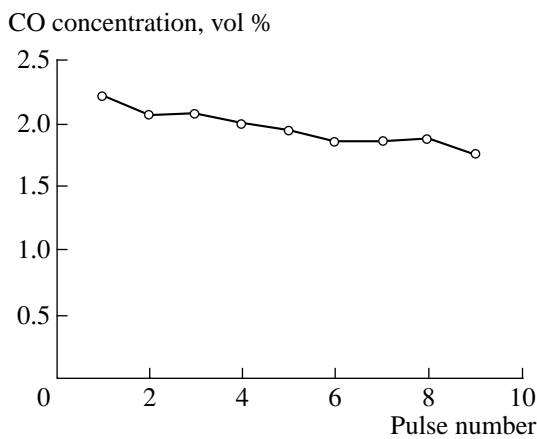


Fig. 5. CO formation in the reaction of Ni/Al<sub>2</sub>O<sub>3</sub> with CO<sub>2</sub> pulses at 700°C.

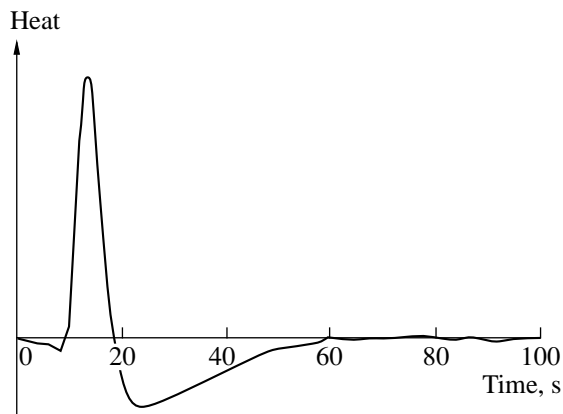


Fig. 6. Thermal effect from the interaction of the CO<sub>2</sub> pulse with the Ni/Al<sub>2</sub>O<sub>3</sub> sample at 700°C.

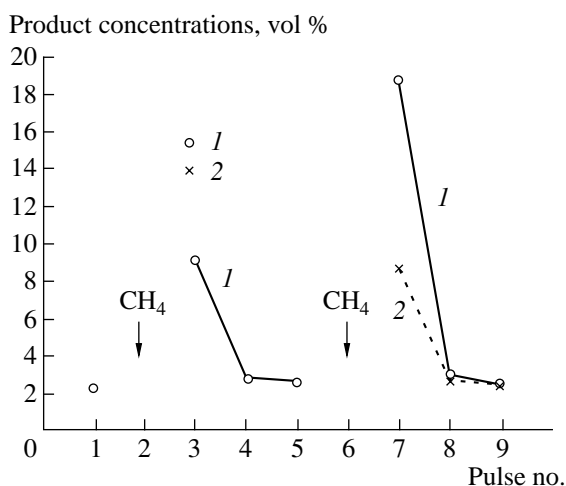


Fig. 7. The concentration of (1) CO and (2) consumption CO<sub>2</sub> in the products of the interaction of CO<sub>2</sub> pulses with Ni/Al<sub>2</sub>O<sub>3</sub> at 700°C and in the case of the alternating pulses of CO<sub>2</sub> (nos. 1, 3–5, and 7–9) and CH<sub>4</sub> (nos. 2 and 6).

data on the formation of CO during a series of pulses: (1) CO<sub>2</sub>, (2) CH<sub>4</sub>, (3–5) CO<sub>2</sub>, (6) CH<sub>4</sub>, and (7–9) CO<sub>2</sub> (only the results of CO<sub>2</sub> pulses are analyzed). The intervals between the pulses lasted 10 min. The reaction of CO<sub>2</sub> with the sample reduced in hydrogen gives only 2% CO. However, in the reaction of the CO<sub>2</sub> pulse with the sample pretreated with a pulse of methane, the yield of CO is an order of magnitude higher. In the case of the CO<sub>2</sub> pulse (no. 7), the amount of CO formed is twice as large as the amount of CO<sub>2</sub> consumed. This means that, under the given conditions, CO<sub>2</sub> rapidly (during one pulse) reacts with carbon formed on nickel in methane decomposition. In further pulses (nos. 8 and 9), CO<sub>2</sub> reacts with the sample in the same way that it reacts with the pure reduced Ni/Al<sub>2</sub>O<sub>3</sub> sample (pulse no. 1).

**Interaction with the pulses of CO, CO<sub>2</sub>, and CO + CO<sub>2</sub>.** To answer the question of whether the equilibrium concentration of CO is achieved during the reaction of a CO<sub>2</sub> pulse with the reduced sample, we studied the interaction of the sample with CO and CO + CO<sub>2</sub> pulses. The results are summarized in Table 2. As can be seen, for the consecutive samples of the same initial composition, the composition of products changed insignificantly. This allows us to consider that, in each separate case, the reactant interacts with the sample in about the same state. For three different initial compositions of reactants, completely different product concentrations are observed. This means that equilibrium is not achieved in reaction (II) under the experimental conditions for the time of one pulse. The concentration of CO equal to ~2% in the reaction of the reduced sample with the CO<sub>2</sub> pulse is not equilibrium, because even when the initial concentration of CO is 2.4%, an additional increase in the concentration of CO is observed at the outlet.

**Interaction with the pulses of CO<sub>2</sub> and O<sub>2</sub>.** In another experiment, we studied the dependence of the rate of CO<sub>2</sub> interaction with the reduced sample on the extent of metallic nickel concentration. The sample was reduced in hydrogen at 700°C and then alternating CO<sub>2</sub> and air pulses were supplied. Figure 8 shows the values of the CO concentration on the amount of oxygen consumed for the catalyst reoxidation. It is seen that the concentration of CO linearly decreases with an increase in the extent of sample oxidation.

**Interaction with the pulses of H<sub>2</sub>.** Figure 9 shows the curves of heat evolution in the interaction of a 10% H<sub>2</sub> + He pulse at 700°C with a sample that was prereduced in a flow of hydrogen at 700°C and then kept in a flow of He at 700°C. We see a relatively fast exothermic effect (0–50 s) and a slower endothermic effect (50–1000 s). The results of chromatographic analyses did not detect any noticeable broadening of a hydrogen peak after its contact with the reduced sample. This means that the apparent endothermic effect is not associated with hydrogen desorption after reversible adsorption on metallic nickel. The reversible adsorption of hydrogen, if any, occurs only during the brief

contact of the sample with a gas pulse. Apparently, the calorimetric signal refers to hydrogen oxidation by catalyst oxygen (exothermic effect) and further water desorption (endothermic effect). The form of this endo-effect allows us to assume that the sample surface preserves hydroxyl groups during the first ~300–400 s after a passing hydrogen pulse.

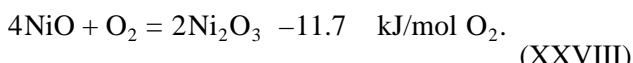
**Interaction with the pulses of  $H_2$  and  $CO_2$ .** To study the effect of adsorbed hydrogen on  $CO_2$  activation, we carried out experiments in which the sample reduced in hydrogen at 700°C was treated with alternating pulses of 10%  $H_2$  + He and  $CO_2$  with different intervals between them. Figure 10 shows the dependence of the amount of CO formed in the reaction with the  $CO_2$  pulse on time elapsed after the 10%  $H_2$  + He pulse. When the time interval was 300 s, the amount of CO formed practically coincided with the amount of CO observed in the reaction of the  $CO_2$  pulse with the reduced sample purged with a flow of helium for several tens of minutes. If the interval between the  $H_2$  and  $CO_2$  pulses is decreased, the amount of CO somewhat increases, but the amount of CO is not increased greater than by a factor of 1.5 with a decrease in the interval down to ~10 s. A further increase in the interval results in a drastic increase in CO formation. However, when the intervals are so short, the initial  $H_2$  and  $CO_2$  pulses overlap noticeably and mix.

## DISCUSSION

### *Methane Activation and Redox Reactions*

Experiments on the reduction and reoxidation of  $Ni/Al_2O_3$  showed that the portion of supported nickel oxide (22%) is capable of being rapidly reduced by hydrogen and reoxidized by air. The fact that the reduction of the rest of nickel oxide is difficult means that oxidized nickel is in at least two states.

The values of the measured oxidation heat  $Q_{ox}$  (see Table 1) can be used for the analysis of the state of supported nickel by comparing with the tabulated values of the enthalpies of reactions  $\Delta H^0$  [11]:



Although the tabulated values refer to reactions in bulk phases, substantial differences in these values of enthalpies allow us to apply them to surface compounds. In our case, the experimental values of  $Q_{ox}$  (Table 1) correspond to the oxidation of metallic nickel to  $NiO$  (reaction (XXVI)), and  $Ni_2O_3$  is not formed under the given condition. At the same time, the formation of  $NiAl_2O_4$  spinel in the reaction between  $NiO$  and  $Al_2O_3$  is possible. Because the heat of the reaction of  $NiAl_2O_4$  synthesis from  $NiO$  and  $Al_2O_3$  is low ( $\Delta H = -2.5 \text{ kJ/mol}$ ), the calorimetric data prevented us from detecting the formation and

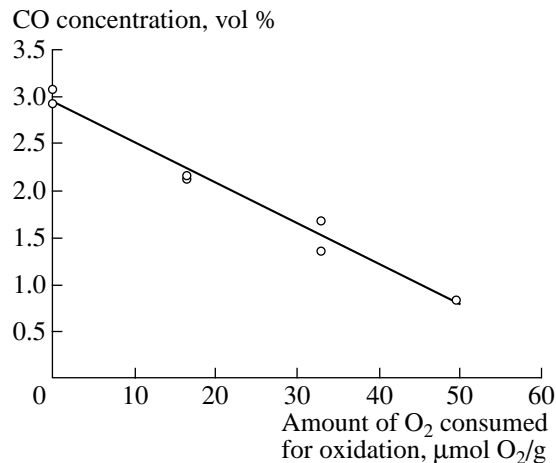


**Fig. 8.** Dependence of the amount of CO in the products of the interaction of  $CO_2$  pulses with reduced  $Ni/Al_2O_3$  on the amount of  $O_2$  consumed for catalyst reoxidation in the case of the alternating pulses of  $CO_2$  and air.

decomposition of aluminate. However, it is expectable that the form of nickel oxide that is hard to reduce is a mixed compound of  $NiO$  and  $Al_2O_3$  (henceforth denoted by  $Ni-Al-O$ ).

**Table 2.** The interaction of  $Ni/Al_2O_3$  with pulses of  $CO$ ,  $CO_2$ , and  $CO + CO_2$

| Pulse number  | Initial pulse composition | CO concentration at the outlet, % | $CO_2$ concentration at the outlet, % |
|---|---------------------------|-----------------------------------|---------------------------------------|
| Sample oxidized in air and reduced in hydrogen at 700°C |                           |                                   |                                       |
| 1   | 100% $CO_2$               | 1.97                              | —*                                    |
| 2   | 100% $CO_2$               | 1.86                              | —                                     |
| 3   | 2.4% $CO + CO_2$          | 3.11                              | —                                     |
| 4   | 2.4% $CO + CO_2$          | 2.99                              | —                                     |
| 5   | 100% $CO_2$               | 1.65                              | —                                     |
| 6   | 100% $CO_2$               | 1.67                              | —                                     |
| 7   | 2.4% $CO + CO_2$          | 2.86                              | —                                     |
| 8   | 2.4% $CO + CO_2$          | 2.9                               | —                                     |
| Sample oxidized in air and reduced in hydrogen at 700°C |                           |                                   |                                       |
| 1   | 100% $CO$                 | —                                 | 7.5                                   |
| 2   | 100% $CO$                 | —                                 | 7.1                                   |
| 3   | 100% $CO$                 | —                                 | 6.6                                   |
| 4   | 100% $CO$                 | —                                 | 6.4                                   |
| 5   | 100% $CO$                 | —                                 | 6.3                                   |
| 6   | 100% $CO$                 | —                                 | 6.9                                   |
| 7   | 100% $CO_2$               | 1.8                               | —                                     |
| 8   | 100% $CO_2$               | 1.5                               | —                                     |

\* A dash means that the concentration of this component was undeterminable in the products.

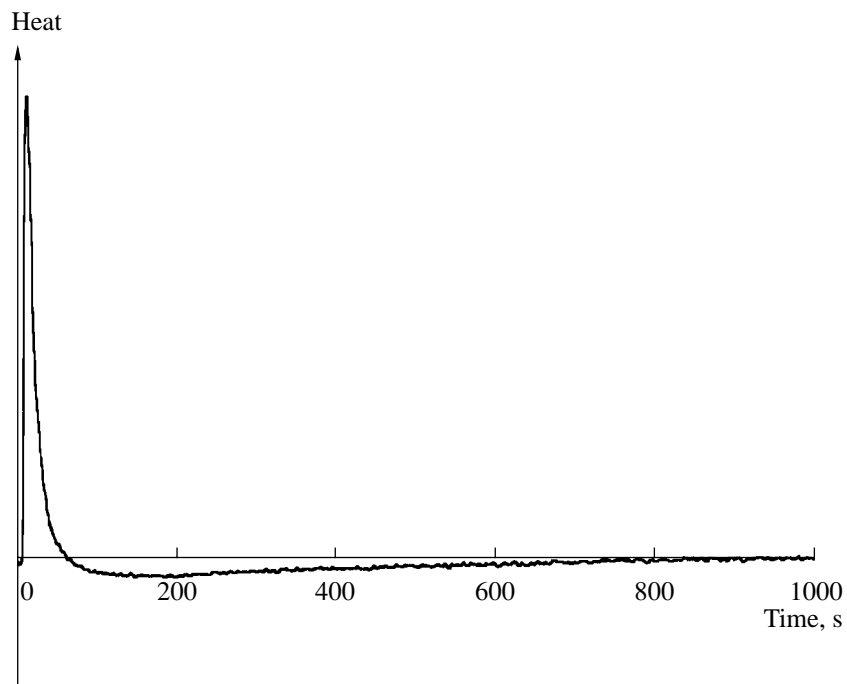


**Fig. 9.** Heat evolution in the reaction between the 10%  $\text{H}_2 + \text{He}$  pulse (700°C) with  $\text{Ni}/\text{Al}_2\text{O}_3$  pretreated first in  $\text{H}_2$  and then in  $\text{He}$  at 700°C.

$\text{Ni}/\text{Al}_2\text{O}_3$  in the completely oxidized state reacts slowly with methane. In this reaction,  $\text{CO}$  and  $\text{H}_2$  are not formed, but the products are  $\text{CO}_2$  and a small amount of ethane. Such a composition of the products corresponds to the well-studied process of the oxidative coupling of methane on oxide systems [9, 12]. In oxidative coupling, methane is commonly considered to be activated by the interaction with surface oxygen via the

Eley–Rideal mechanism to form a methyl radical and a hydroxyl group [12]:



where the subscript s refers to the surface species.

The absence of  $\text{H}_2$  in the products means that the dissociative adsorption of methane (reaction (I)) is only possible in the presence of metallic nickel. The initial rate of its formation via supported nickel oxide reduction by methane is very low, and this reaction is completely suppressed in the presence of gaseous oxygen. However, after the formation of metallic nickel, almost immediate nickel oxide reduction takes place and reaction (I) accelerates (see Fig. 1).

On the contrary, the rate of methane interaction with reduced  $\text{Ni}/\text{Al}_2\text{O}_3$  is high (Fig. 3). The conversion of methane in the reaction of methane pulses with reduced  $\text{Ni}/\text{Al}_2\text{O}_3$  (~50%) is close to methane conversion in the case of  $\text{CH}_4 + \text{CO}_2$  pulses (~65%). This supports the opinion [1, 2] that the dissociative adsorption of methane on metallic nickel is the main route of methane activation in carbon dioxide reforming.

The results of methane pulse interaction with the reduced  $\text{Ni}/\text{Al}_2\text{O}_3$  (Fig. 3) sample shows that the products of methane chemisorption react with lattice oxygen, which remains in the sample after treatment with hydrogen.  $\text{CO}$  and  $\text{H}_2$  are also formed in this case, as is evident from the fact that the yield of  $\text{H}_2$  is maximal in the first pulse of methane:

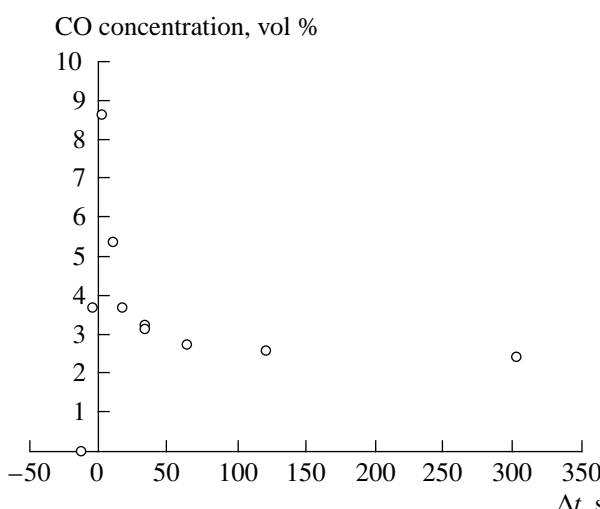


**Fig. 10.** Dependence of the amount of  $\text{CO}$  formed in the reaction of the  $\text{CO}_2$  pulse with  $\text{Ni}/\text{Al}_2\text{O}_3$  on the interval  $\Delta t$  between the pulses of 10%  $\text{H}_2 + \text{He}$  and 100%  $\text{CO}_2$ .

The retention time and broadening of the CO peak in the chromatogram point to the lower rate of reaction (XXX) compared to reaction (I). It is likely that reaction (XXX) is accompanied by surface diffusion between nickel crystallites and the barely reducible Ni-Al-O phase. This also retards reaction (XXX).

Data presented in Fig. 3 show that the initial conversion of methane, which is almost constant, starts to decrease after six or seven pulses. This decrease takes place when the evolution of CO discontinues in the oxidation of products of methane decomposition by reaction (XXX). Obviously, a decrease in the methane conversion is due to nickel surface coking under the conditions when active lattice oxygen, which is able to remove coke, is exhausted. This means that the participation of lattice oxygen of Ni/Al<sub>2</sub>O<sub>3</sub> in methane oxidation prevents catalyst coking.

In general, we find that the interaction of methane chemisorption products with lattice oxygen creates a new route for methane activation in methane reforming with carbon dioxide, but the rates of CO and H<sub>2</sub> formation via this route do not increase noticeably the overall rate of reforming. At the same time the positive role of reaction (XXX) is that it increases the extent of nickel oxide reduction and decreases the rate of coking. It is possible that the routes of methane activation proposed in [6, 7] that include the participation of transition metal (chromium or cerium) oxides also affect the rate of reforming by changing the catalyst state.

Another situation appears when oxygen adsorption from the gas phase fills up active oxygen species right on the nickel surface (Fig. 2, pulse nos. 8 and 12). This oxygen can rapidly react with adsorbed methane. If its amount constitutes at least 60% of oxygen required for the complete reoxidation of reduced Ni/Al<sub>2</sub>O<sub>3</sub>, then this oxygen noticeably increases rather than decreases the conversion of methane. When the extent of reoxidation is medium (20%), an increase in the hydrogen yield is also observed. Oxygen adsorbed on nickel creates an important route for methane activation in carbon dioxide reforming and allows the inclusion of steps similar to (VII) in the mechanism of reforming.

Tomishige *et al.* [13] assumed that the apparent decrease in the activity of the Ni<sub>0.03</sub>Mg<sub>0.97</sub>O catalyst with time is due to the partial reoxidation of nickel crystallites. Our data suggest that in the case of Ni/Al<sub>2</sub>O<sub>3</sub> even the substantial reoxidation of reduced nickel does not itself decrease the rate of methane activation.

### CO<sub>2</sub> Activation

Data on the interaction of Ni/Al<sub>2</sub>O<sub>3</sub> with CO<sub>2</sub> pulses suggest that both the reversible adsorption of CO<sub>2</sub> (Fig. 6) and dissociative adsorption by reaction (II) (Fig. 5) occur in the system under study. The apparent characteristic lifetime of reversibly adsorbed CO<sub>2</sub> is ~20–30 s. The amount of reversibly adsorbed CO<sub>2</sub> is

independent of the extent of nickel oxide reduction. That is, the reversible adsorption of CO<sub>2</sub> is insensitive to the nickel oxidation state in the sample.

On the contrary, the reduction of CO<sub>2</sub> to CO (reaction (II)) only occurs on metallic nickel and leads to nickel oxidation (Fig. 5). This means that reaction (II) is one of the routes of CO<sub>2</sub> activation in methane reforming with carbon dioxide, which agrees with the assumption of many researchers [1, 2]. However, the conversion of CO<sub>2</sub> in our experiments was at most 2.0–2.2%. In the case of CH<sub>4</sub> + CO<sub>2</sub> pulses under analogous conditions, the conversion of CO<sub>2</sub> was much higher 85%. The results of reduced Ni/Al<sub>2</sub>O<sub>3</sub> interaction with pulses of CO<sub>2</sub>, CO, and CO + CO<sub>2</sub> suggest that 2% conversion in the reaction of CO<sub>2</sub> with Ni/Al<sub>2</sub>O<sub>3</sub> is not the result of achieving the equilibrium CO/CO<sub>2</sub> ratio. The amount of reduced CO<sub>2</sub> was not restricted by the number of surface atoms on the particles of metallic nickel. This is evident from the fact that ten times more O<sub>2</sub> molecules (20% in the initial pulse and 95% conversion) reacted with the nickel surface than CO<sub>2</sub> molecules did (100% CO<sub>2</sub> in the initial pulse and 2% conversion) when the reduced sample was treated by a pulse of air under analogous conditions (Table 1). Therefore, our data point to the relatively low rate of reaction (II).

Data shown in Fig. 8 suggest that the yield of CO in CO<sub>2</sub> reduction by nickel linearly decreases with an increase in the extent of nickel oxide reduction. This dependence should be observed if the concentration of CO is determined by the rate of its formation according to the rate law  $w_{CO} = kP_{CO_2} [Ni]_s$ . In the case of the equilibrium formation of CO, a strong nonlinear dependence of the CO concentration on the extent of reduced nickel reoxidation is expectable.

Thus, we conclude that the rate of reaction (II) in the Ni/Al<sub>2</sub>O<sub>3</sub> system cannot provide the rate of CO<sub>2</sub> activation observed in the process of methane reforming with carbon dioxide and that reaction (II) is not the main route of CO<sub>2</sub> activation.

Experiments with CO<sub>2</sub> pulses and the Ni/Al<sub>2</sub>O<sub>3</sub> catalyst reduced by methane pulses showed that the much higher yield of CO and CO<sub>2</sub> conversion are observed in this case. The Ni/Al<sub>2</sub>O<sub>3</sub> sample after reaction (I) contains surface carbon (and possibly CH<sub>x</sub> fragments), which reacted with CO<sub>2</sub> by reaction (V). Figure 7 shows that, in three-pulse series, the yield of CO in the second and third pulses of CO<sub>2</sub> was practically equal to the yield of CO after the reaction of CO<sub>2</sub> with the Ni/Al<sub>2</sub>O<sub>3</sub> sample before the contact with methane. This means that surface carbon entirely reacts during one CO<sub>2</sub> pulse and that reaction (V) is fast. It is likely that this reaction is the main route of CO<sub>2</sub> activation in the methane reforming with carbon dioxide on Ni/Al<sub>2</sub>O<sub>3</sub>. This conclusion agrees well with that drawn by Chen *et al.* [14] who showed that one of the forms of surface carbon ( $\alpha$ -carbon) is an intermediate species in the methane reforming with carbon dioxide on Ni<sub>x</sub>Mg<sub>1-x</sub>O catalysts.

As follows from Fig. 2, the partial reoxidation of Ni/Al<sub>2</sub>O<sub>3</sub> leads to a strong decrease in the conversion of CO<sub>2</sub> from 85 to 60% when the extent of reoxidation was 20% (pulse no. 8) and to 0.6% when the extent of reoxidation was 60%. Obviously, a decrease in the rate of CO<sub>2</sub> activation is due to the competition of CO<sub>2</sub> and adsorbed oxygen in the reaction with surface carbon. We conclude that the fast oxidation of surface carbon to CO<sub>2</sub>, rather than a decrease in the fraction of metallic nickel and the proportional decrease in the rates of methane and CO<sub>2</sub> activation by reactions (I) and (II), is the reason for Ni-containing catalyst poisoning in the presence of gas-phase oxygen.

The process of CO<sub>2</sub> activation by reaction (XIII) is more difficult to study. The analysis of hydrogen pulse interaction with Ni/Al<sub>2</sub>O<sub>3</sub> (Fig. 9) led us to conclude that the form of adsorption H<sub>2,ad</sub> exists only in contact with gaseous hydrogen, and hydroxyl groups remain on the Ni/Al<sub>2</sub>O<sub>3</sub> surface for 200–300 s after the hydrogen pulse. Data on the dependence of the CO yield on the time interval between the pulses of H<sub>2</sub> and CO<sub>2</sub> (Fig. 10) showed that a decrease in the interval from 300 to 30 s results in a very small increase in the CO yield. This means that the surface hydroxyl groups do not affect the activation of CO<sub>2</sub>. A drastic increase in the yield of CO is only observed when the interval between the pulses of H<sub>2</sub> and CO<sub>2</sub> is very short (<10 s) and gas pulses overlap and mix. It is probable that in this case reaction (XIII) occurs. This led us to conclude that reaction (XIII) is another important route of CO<sub>2</sub> activation in methane reforming with carbon dioxide.

## CONCLUSION

The main route of methane reforming with carbon dioxide on Ni/Al<sub>2</sub>O<sub>3</sub> is the dissociative adsorption of CH<sub>4</sub> with the formation of surface carbon and H<sub>2</sub>. This carbon reacts with CO<sub>2</sub> to form CO by the reverse Boudouard reaction. Side routes are the interaction of the products of methane chemisorption with lattice oxygen of the catalyst and the reduction of CO<sub>2</sub> by metallic nickel. The competitive reaction of the complete oxidation of surface carbon by adsorbed oxygen leads to a decrease in the conversion of CO<sub>2</sub> in methane reforming with carbon dioxide. Therefore, the presence of gaseous oxygen in the reaction mixture results in a

decrease in the rate of reforming (catalyst poisoning by oxygen).

## ACKNOWLEDGMENTS

We thank O.V. Isaev for catalyst preparation, P.A. Shiryaev for obtaining XRD spectra, and Z.T. Fat-takhova for measuring the specific surface area. This work was supported by the Russian Foundation for Basic Research (project no. 98-03-32183) and the Japanese program NEDO (project no. 98EA4 DME POWER).

## REFERENCES

1. Bradford, M.C.J. and Vannice, M.A., *Catal. Rev. – Sci. Eng.*, 1999, vol. 41, no. 1, p. 1.
2. Krylov, O.V., *Ross. Khim. Zh.*, 2000, vol. 44, no. 1, p. 19.
3. Mark, M.F. and Maier, W.F., *J. Catal.*, 1996, vol. 164, no. 1, p. 122.
4. Hei, M.J., Chen, H.B., Yi, J., Lin, Y.J., Lin, Y.Z., Wei, G., and Liao, D.W., *Surf. Sci.*, 1998, vol. 417, no. 1, p. 82.
5. Slagtern, A., Schuurman, Y., Leclercq, C., Verykios, X., and Mirodatos, C., *J. Catal.*, 1997, vol. 172, p. 118.
6. Isaev, O.V., Korchak, V.N., Krylov, O.V., Firsova, A.A., Tyulenin, Yu.P., and Shashkin, D.P., *Kinet. Katal.*, (in press).
7. Zhang, O. and Otsuka, K., *Chem. Lett.*, 1993, p. 363.
8. Bychkov, V.Yu., Sinev, M.Yu., Korchak, V.N., Aptekar', E.L., and Krylov, O.V., *Kinet. Katal.*, 1986, vol. 27, no. 5, p. 1190.
9. Bychkov, V.Yu., Sinev, M.Yu., Korchak, V.N., Aptekar', E.L., and Krylov, O.V., *Kinet. Katal.*, 1989, vol. 30, no. 5, p. 1137.
10. Sinev, M.Yu. and Bychkov, V.Yu., *Kinet. Katal.*, 1999, vol. 40, no. 6, p. 906.
11. *Termicheskie konstanty veshchestv* (Thermal Constants of Substances), Moscow: VINITI, 1965–1974, nos. 1–7.
12. Arutyunov, V.S. and Krylov, O.V., *Okislitel'nye prevrashcheniya metana* (Oxidative Conversion of Methane), Moscow: Nauka, 1998.
13. Tomishige, K., Chen, Y., Yamazaki, O., Himeno, Y., Koganezawa, Y., and Fujimoto, K., *Stud. Surf. Sci. Catal.*, 1998, vol. 119, p. 861.
14. Chen, Y.-G., Tomishige, K., and Fujimoto, K., *Appl. Catal., A*, 1997, vol. 161, p. L11.